Title
Superconducting undulators with variable polarization and enhanced spectral range

Journal
IEEE Transactions on Applied Superconductivity, 16(2)

ISSN
1051-8223

Authors
Prestemon, S
Schlueter, R
Marks, S
et al.

Publication Date
2006-06-01

DOI
10.1109/TASC.2006.871262

Peer reviewed

Superconducting Undulators With Variable Polarization and Enhanced Spectral Range

S. Prestemon, R. Schlueter, S. Marks, and D. R. Dietderich

***Abstract*—A concept utilizing superconducting magnets for variable polarization insertion devices is presented. The iron-free design enables full variable linear and elliptical polarization over a broad spectral range. With appropriate electrical switching the same device can access higher energies through period-halving, while continuing to provide variable-linear polarization; furthermore, separate switching will allow for period-doubling with full linear and elliptical polarization control. The performance, both in terms of field/spectral performance and in terms of polarization control, is compared to existing permanent magnet EPU devices. Engineering issues associated with the fabrication and implementation of the device are discussed.**

***Index Terms*—Polarization, superconducting undulators.**

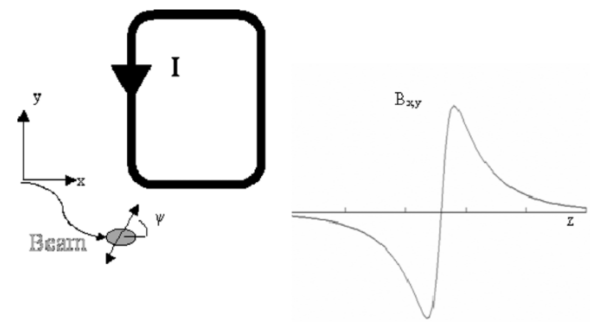

Fig. 1. The B_x and B_y fields along the z axis, emanating from a current loop in the first quadrant of the x-y plane. The field vector lies on a symmetry plane of angle ψ to the x-axis.

I. Introduction

Over the past few years there has been renewed interest in developing superconducting undulator (SCU) technology for planar devices, motivated by the promise of increased spectral brightness and/or enhanced spectral range (or, equivalently, access to higher photon energy while maintaining harmonic overlap). It is worth noting that the first undulator designs were helical SCUs, and in fact were designed to generate circular polarization [1]–[3]; the very successful development of permanent magnet insertion devices in the 1980s [4], [5] largely superseded that of electromagnetic wigglers and helical SCUs. Improvements in superconductor performance and a thirst for brightness and energy range have fueled the renewed interest in SCUs [6].

The development of pure permanent magnet elliptically polarizing undulators (EPU) has had a significant impact on the type of science that can be addressed with synchrotron radiation. As the interest in polarization control grows, it is worth investigating alternative techniques to the generation of polarized undulator radiation that may provide enhanced performance for certain applications, defined for example in terms of brightness and/or spectral range.

A number of concepts have recently been proposed that use superconducting devices to provide variable polarization [6]–[8]. To date, the approaches have relied on hybrid (i.e. iron-yoke based techniques) that super-impose tilted planar fields. Here we present a novel approach that foregoes iron and can provide significantly enhanced spectral range as compared to other superconducting and permanent magnet EPU (PM-EPU) concepts.

In Section II we provide the basic concept for the superconducting EPU (SC-EPU) design, including the magnetic design and details of the polarization control permitted, as well as the means by which the spectral range can be significantly enhanced. In Section III we discuss R&D issues that must be overcome, including those that are already of concern (and to some degree being addressed) with planar SCU devices as well as issues particular to SC-EPUs.

In Section IV we provide a sample of the performance that can be anticipated from an SC-EPU compared to a PM-EPU for the Advanced Light Source (ALS), and the strengths and weaknesses of the two technologies are outlined.

II. Variable-Polarization Control

A. Basic Concepts

The field vector at any point in space, generated by a line current of finite length, can be easily calculated using the Biot-Savart formula. We consider a simple rectangular loop located in the first quadrant of the x-y plane, and assume the beam is traveling in the z direction, centered at $x = y = 0$. The Bx and By vector components seen by the beam are qualitatively outlined in Fig. 1.

An axial array of such coaxial loops with alternating current direction will result in a sinusoidal B_x and B_y field profile (see Fig. 2). The field vector will lie on a symmetry plane (see Fig. 1) with angle ψ to the x-axis, defined by the loop geometry with respect to the z axis.

B. Multiple Quadrants and Polarization Control

We now consider a four-quadrant array of current-loop ("coil") series (see Fig. 3). The quadrants will be labeled A, B, C, and D, and we assume coils C and D are obtained from A and B via π-rotation, respectively. The field vectors from the A

Manuscript received September 20, 2005. This work was supported by the U. S. Department of Energy, under Contract DE-AC02-05CH11231.

The authors are with the Lawrence Berkeley National Laboratory, Berkeley, CA USA (e-mail: soprestemon@lbl.gov; drdieterich@lbl.gov; s_marks@lbl.gov; rdschlueter@lbl.gov).

Digital Object Identifier 10.1109/TASC.2006.871262

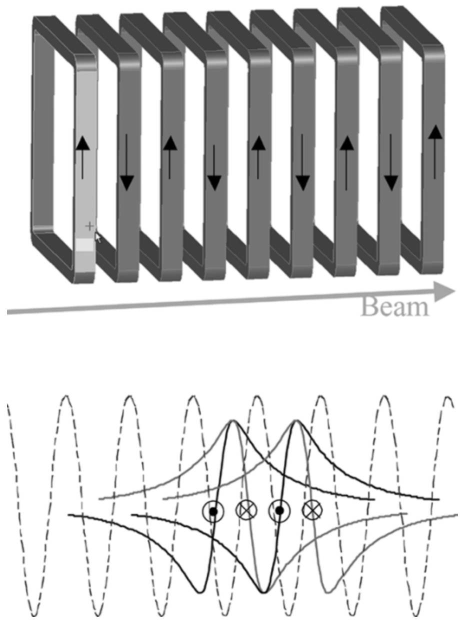

Fig. 2. A series of current loops of alternating current direction results in a sinusoidal field on the z-axis.

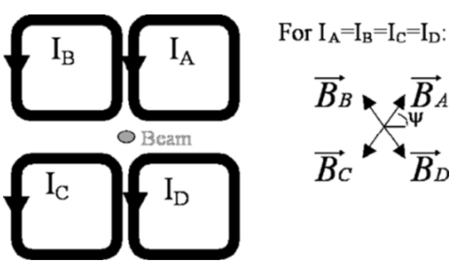

Fig. 3. Four quadrants of identical arrays provides access to two independent field orientations; independent control via two separate power supplies yields variable linear polarization control.

and C quadrants will therefore be situated on the same plane, as will the fields from the B and D coils. By correctly directing the currents in C with respect to the A coils ($I_A = -I_C$ in Fig. 3) their fields will be additive; the same can be said for B and D coils. Since the field vectors at an arbitrary axial location z_0 generated by I_A is linearly independent of that generated by I_B, control of (I_A, I_B) provides full linear polarization control, i.e. $\vec{B}$ can be forced to lie on a plane of arbitrary angle ψ with respect to the x-axis, and the resulting electric field generated by passing relativistic electrons will therefore be of associated linear polarization. For example, setting $I_A = I_B$ results in vertical field, i.e. horizontal polarization.

C. Duplicate Phase-Shifted Arrays for Elliptic Polarization

The generation of elliptical polarization requires that the B_x and B_y fields be out of phase in z. This can be accomplished by interlacing a duplicate array of coil-series, as shown in Fig. 4. For clarity, we distinguish the original and phase shifted arrays by superscripts α and β respectively. Note that the fields generated by I_A^α and I_A^β are out of phase by $\pi/2$ (the same applies for

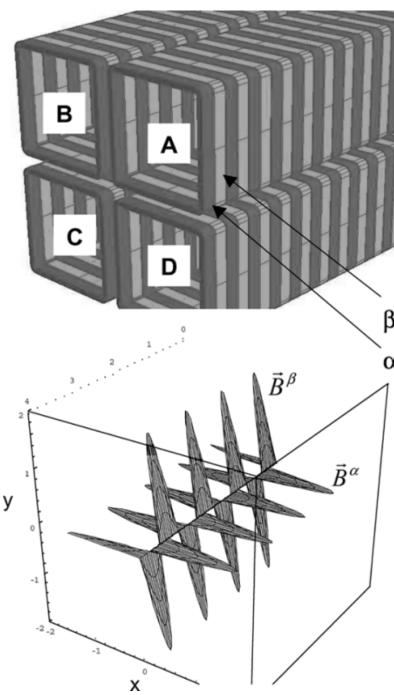

Fig. 4. Two interlaced sets (α and β) of four-quadrant coil arrays (see top sketch), operated with four power supplies, can provide full variable linear and elliptic polarization control. As an example, the bottom figure maps the α and β fields for a case where the two planar fields are defined to be orthogonal, yielding variable elliptic polarization by varying the relative field strengths.

the B arrays). The fields generated by the α and β arrays can be expressed as

$$\vec{B}^\alpha\left(I_A^\alpha, I_B^\alpha; z\right) \quad \vec{B}^\beta\left(I_A^\beta, I_B^\beta; z\right) \tag{1}$$

with the simple relations

$$\begin{aligned}\begin{pmatrix} B_x^\alpha \\ B_y^\alpha \end{pmatrix} &= \eta\left\{\begin{pmatrix} \mathrm{Cos}(\psi) & -\mathrm{Cos}(\psi) \\ \mathrm{Sin}(\psi) & \mathrm{Sin}(\psi) \end{pmatrix}\begin{pmatrix} I_A^\alpha \\ I_B^\alpha \end{pmatrix}\right\} \\ &\quad \times \mathrm{Sin}\left(\frac{2\pi z}{\lambda}\right) \\ \begin{pmatrix} B_x^\beta \\ B_y^\beta \end{pmatrix} &= \eta\left\{\begin{pmatrix} \mathrm{Cos}(\psi) & -\mathrm{Cos}(\psi) \\ \mathrm{Sin}(\psi) & \mathrm{Sin}(\psi) \end{pmatrix}\begin{pmatrix} I_A^\beta \\ I_B^\beta \end{pmatrix}\right\} \\ &\quad \times \mathrm{Sin}\left(\frac{2\pi z}{\lambda} - \frac{\pi}{2}\right)\end{aligned} \tag{2}$$

where λ is the period, η a geometric scale factor and ψ is the geometry-induced angle described in Fig. 1. Note that both the α and β arrays are independently capable of full variable linear polarization. Aligning their field vectors, say in vertical field mode, results in an enhanced field strength vertical field, phase shifted by $\pi/4$ with respect to the α field. It is also readily apparent that all elliptic polarization modes are accessible; the major/minor axis can be arbitrarily positioned by varying the four currents

$$I_A^\alpha, I_B^\alpha, I_A^\beta, I_B^\beta.$$

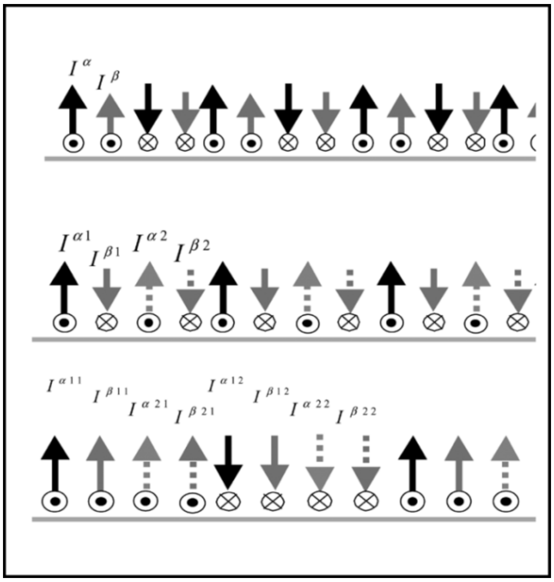

Fig. 5. The basic coil circuitry is shown in the top figure. The α and β coil sets are independently controlled. Reconfiguring the coil circuitry allows for period halving [second figure; see (4) for current-constraints]. Further segregating the coil circuitry allows for a period-doubling configuration [lower figure; see (5)]. The solid and dotted arrows in the lower figure indicate the new $\pi/2$ phase-shifted coils that can be used to provide polarization control in the 2λ mode.

D. Modified Circuitry to Period-Double and Period-Halve

The basic α set of coils in the upper sketch of Fig. 4 yield a field of period λ, as do the β coils. We now connect every other coil in the α set in one series $\alpha 1$, and the others in a series $\alpha 2$; the same connections are applied to the β series (see Fig. 5). Setting

$$I_{A,B}^{\alpha 2} = -I_{A,B}^{\alpha 1} \quad I_{A,B}^{\beta 2} = -I_{A,B}^{\beta 1} \tag{3}$$

for example, yields the λ-period, full polarization control scenario discussed previously. We can change the configuration to

$$I_{A,B}^{\alpha 2} = I_{A,B}^{\alpha 1} \quad I_{A,B}^{\beta 2} = I_{A,B}^{\beta 1} = -I_{A,B}^{\alpha 1} \tag{4}$$

resulting in a field of period $\lambda/2$. Note that the β coil currents are now in series with the α coils; i.e. in the period-halved configuration only variable linear polarization can be obtained (the A and B independent field vectors, controlled by $I_A^{\alpha 1}, I_B^{\alpha 1}$, are still available).

Perhaps more interestingly, a further decomposition of the coil circuitry, illustrated in the bottom sketch in Fig. 5, allows for period doubling using the circuit constraints

$$\begin{aligned} I_{A,B}^{\beta 11} &= -I_{A,B}^{\alpha 12} = -I_{A,B}^{\beta 12} = I_{A,B}^{\alpha 11} \\ I_{A,B}^{\beta 21} &= -I_{A,B}^{\alpha 22} = -I_{A,B}^{\beta 22} = I_{A,B}^{\alpha 21} \end{aligned} \tag{5}$$

Independent control of the four currents $I_A^{\alpha 11}, I_B^{\alpha 11}, I_A^{\alpha 21}, I_B^{\alpha 21}$ provides full linear and elliptic polarization control at 2λ period.

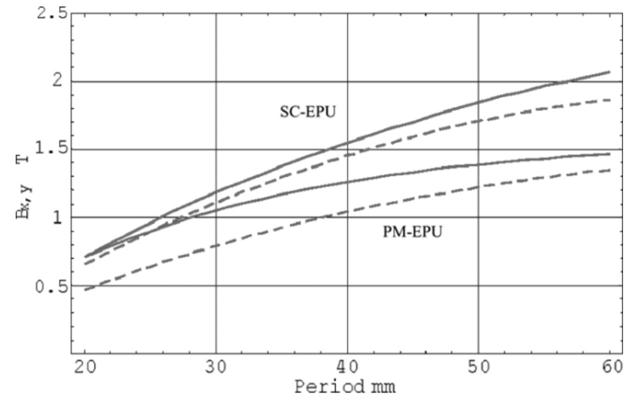

Fig. 6. Field vs period for SC-EPU and PM-EPU designs in linear horizontal (solid) and linear vertical (dotted) modes.

III. R&D Issues

A number of issues have previously been identified that must be addressed before superconducting undulators can be considered a mature technology, comparable to pure and hybrid technologies [6]. These include image-current heating and other beam-based heat sources and the associated cryogenic considerations; cold magnetic measurements with sufficient precision to determine phase errors; and a method to compensate for magnetic errors.

The SC-EPU concept outlined here must also address EPU-specific issues. Three key concerns are 1) ramp-rate limitations associated with superconductor AC-losses 2) beam dynamics considerations, which have become a serious issue for PM-EPU devices operating on low-energy rings in top-off mode [9], and 3) technical issues associated with switching between $\lambda/2$, λ, and 2λ operational modes. The ramp-rate issue can be partially addressed by selecting/specifying a superconductor that minimizes the AC-losses (i.e. the heat generated during ramping), incorporating design features in the system that provide a mechanism to extract the heat out to the cooling system, and providing sufficient temperature margin in the design to allow for some temperature excursions.

The beam dynamics issue has not been addressed as yet. Investigations are currently in progress at the ALS and elsewhere on modeling the nonlinear dynamics of PM-EPUs, and providing magnetic corrections. We anticipate that the work can be applied to SC-EPU designs as well.

IV. Performance Characteristics

The performance of a candidate SC-EPU design can be evaluated rather expeditiously due to the linear field-current relation (see (2)) and the precise and fast integration that is possible for the Biot-Savart formulas. For a given geometry and polarization (i.e. current distribution) a single calculation is made. The on-axis field $\vec{B}(z)$ and the peak fields seen by different coil-packs are then determined. The intercept of the (linear) peak field load line and the conductor $J_{c}(B)$ curve provides the magnets peak current, and hence the peak performance is readily obtained.

To illustrate the potential performance of an SC-EPU, we first compare anticipated field versus period curves for SC-EPUs and

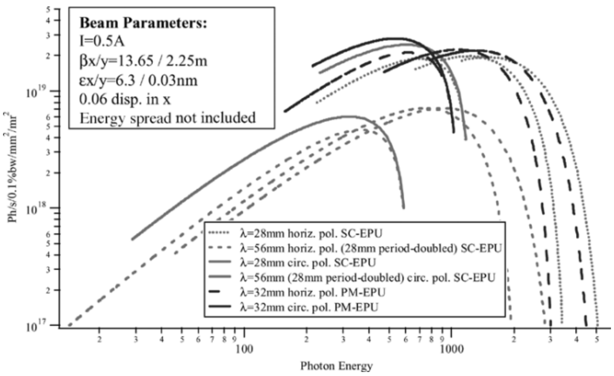

Fig. 7. Brightness plot of an SC-EPU and an PM-EPU. Note that the performance of the devices is nearly identical in the λ-mode; the SC-EPU can deliver photons at significantly lower energy via the 2λ-mode. In the case of linear polarization, 1st, 3rd and 5th harmonics are shown.

PM-EPUs (see Fig. 6) for a vacuum gap of 5 mm; the corresponding magnetic gaps used for the calculations are 6.6 mm and 7.3 mm, respectively. We assume $\mathrm{Nb_3Sn}$ superconductor, as described in [10], [11]. We then compare spectral brightness for two devices reaching the same minimum photon energy, a 30 mm period PM-EPU and a 27 mm period SC-EPU (see Fig. 7). ALS upgrade beam parameters (shown in the figure) are used. For fairness, the SC-EPU is assumed to be 40 mm shorter than the PM-EPU to account for thermal end transitions. Note that the two devices yield essentially identical performance over the core photon energies. The period doubled SC-EPU, however, yields significantly enhanced spectral range, extending down at least one more decade. For this example device the period-halved mode is limited to K $\sim$ 0.5 and is therefore not of interest.

The SC-EPU concept presented here may be of interest to users requiring a broad spectral range of full variable polarization control, without sacrificing brightness as compared to existing EPU devices.

REFERENCES

[1] D. F. Alferov, Y. A. Bashmakov, and E. G. Bessanov, *Sov. Phys. Tech. Phys.*, vol. 18, no. 10, Apr. 1974.
[2] L. R. Elias *et al., Phys. Rev. Lett.*, vol. 36, p. 717, 1976.
[3] B. M. Kincaid, *J. Appl. Phys.*, vol. 48, no. 7, Jul. 1977.
[4] K. Halbach, *Nuclear Instr. and Meth.*, vol. 187, pp. 109–117, 1981.
[5] ——, "ID Design," LBNL Report V-8811-1.1-16, 1989.
[6] *Proc. Workshop on Superconducting Undulators & Wigglers*. Grenoble, 30 Jun.–1st Jul. 2003 [Online]. Available: http://www.esrf.fr/Accelerators/Conferences/ID_Workshop
[7] B. Kostka *et al.*, "Superconductive undulators with variable polarization direction," *IEEE Trans. Appl. Supercond.*, presented at *APAC 2004,* Geongju, Korea, Mar. 2004.
[8] S. Chouhan, D. Harder, G. Rakowsky, J. Skaritka, and T. Tanabe, "Research & development of a variable polarization superconducting undulator at the NSLS," in *Proc. PAC 2005*.
[9] C. Steier, S. Marks, S. Prestemon, D. Robin, R. Schlueter, and A. Wolski, "Study of row-phase dependent skew quadrupoles in Apple-II type EPUs at the ALS," in *Proc. of EPAC 2004*, Lucerne, Switzerland.
[10] S. Prestemon, D. Dietderich, S. Marks, and R. Schlueter, "NbTi and $\mathrm{Nb_3Sn}$ superconducting undulator designs," in *Proc. 8th Int. Conf.*, Aug. 25–29, 2003.
[11] R. D. Schlueter, S. Marks, S. Prestemon, and D. Dietderich, "Superconducting undulator research at LBNL," *Synchrotron Radiation News*, vol. 17, no. 1, 2004.